

The strength of the electroweak phase transition at $m_H \approx 80$ GeV

F. Csikor

*Institute for Theoretical Physics, Eötvös University,
H-1088 Budapest, Hungary*

Z. Fodor*

KEK, Theory Group, 1-1 Oho, Tsukuba 305, Japan

J. Heitger†

*Institut für Theoretische Physik I, Universität Münster,
D-48149 Münster, Germany*

Abstract

In this letter we present the results of our numerical simulations for the finite temperature electroweak phase transition using the SU(2)-Higgs model on four-dimensional lattices at $m_H \approx 80$ GeV. The temporal extension $L_t = 2$ is used for asymmetric lattice spacings with an asymmetry parameter $a_s/a_t \approx 4$. The measured thermodynamical quantities (interface tension, jump of the order parameter and latent heat) suggest that the phase transition is of very weakly first order.

PACS Numbers: 11.15.Ha, 12.15.-y

arXiv:hep-lat/9807021v2 12 Jan 1999

*On leave from Institute for Theoretical Physics, Eötvös University, H-1088 Budapest, Hungary

†Present address: DESY, Platanenallee 6, D-15738 Zeuthen, Germany

1 Introduction

The standard picture of the electroweak theory tells us that at high temperatures (in the early universe) the electroweak symmetry is restored. As the universe expands and cools down, there is a phase transition between the high temperature “symmetric” and the low temperature “broken” phases. The rate of the baryon violating sphaleron processes is unsuppressed at high temperatures and is basically frozen in the low temperature phase. As a consequence, the presently observed cosmological baryon asymmetry has been finally determined at the electroweak phase transition [1].

In order to clarify the details of this phase transition several techniques have been used. Since the bosonic fields have bad infrared behaviour in the perturbative approach [2, 3, 4], several nonperturbative approaches have been applied to solve the problem. The most promising one is the use of lattice simulations. Two main strategies are used to analyze the problem on the lattice.

One of them is to use four-dimensional lattices and study the phase transition and its thermodynamical properties there. Since the bad infrared behaviour is connected to the bosonic fields only, the SU(2)-Higgs model is analyzed [5, 6], and the fermionic sector is included by perturbative steps. It has been shown that the finite temperature electroweak phase transition is of first order for Higgs boson masses around and below 50 GeV. The strength of the phase transition rapidly decreases as m_H increases.

The other possibility contains a systematic combination of perturbative and non-perturbative methods. One starts with the original theory (e.g. the Standard Model) and integrates out the heavy degrees of freedom perturbatively. The obtained theory is a three-dimensional bosonic one (e.g. SU(2)-Higgs or SU(2) \times U(1)-Higgs) [7].

Analyzing the finite temperature electroweak phase transition by these two different approaches, thus in four and three dimensions, provides not only a useful cross-check between them, but the comparison of the results also reveals a lot about the applicability of the perturbative reduction techniques. Since none of the lattice results contains the fermions, the fermionic sector has to be included perturbatively. This would be completely analogous to the perturbative dimensional reduction step for the heavy bosonic modes.

There has been a lot of speculations that the first order nature of the electroweak phase transition disappears for large Higgs boson masses (about 80-90 GeV). According to $L_t = 2$, four-dimensional results with finite-size analysis there is a first order phase transition for Higgs boson masses of 66 GeV, but no sign of a first order phase transition could be observed for masses larger than 85 GeV (last paper in [5]). Recently, in the three-dimensional theory the endpoint of the phase transition has been determined [8]. Using the same gauge coupling as in the four-dimensional approaches, no first order phase transition exists for Higgs boson masses above ~ 65 GeV.

It is of essential importance to clarify the relationship between the full four-dimensional results and the reduced three-dimensional ones. For this purpose the analysis of the order of the phase transition between 65 GeV and 85 GeV Higgs boson masses in the former case is a particularly sensitive possibility. The expected shift of the endpoint compared to three dimensions may give informations about the overall uncertainties of the reduction procedure.

In this letter we present the results of our numerical simulations for the finite temperature electroweak phase transition using the SU(2)-Higgs model on four-dimensional lattices at $m_H \approx 80$ GeV. The temporal extension $L_t = 2$ is used for asymmetric lattice spacings with an asymmetry parameter $a_s/a_t \approx 4$. The measured thermodynamical quantities (interface tension, jump of the order parameter and latent heat) suggest that the phase transition is of very weakly first order. Section 2 gives our definitions and some details of the simulations. Section 3 contains the analysis of the thermodynamical quantities, while Section 4 presents an estimate of the endpoint for the finite temperature electroweak phase transition. In Section 5 we summarize our results and give an outlook.

2 Lattice formulation and simulation

We will study the four-dimensional SU(2)-Higgs lattice model for $L_t = 2$ temporal extensions. Since the phase transition is supposed to be quite weak, we need large physical volumes in the simulations. The temporal lattice spacing in physical units is set by the critical temperature of the phase transition, $a_t = 1/(T_c L_t)$. A large physical volume is ensured by a different choice for the spatial lattice spacing $a_s > a_t$. The asymmetric lattice spacing scenario can be induced by choosing different coupling strengths in the action for time-like and space-like directions. The action reads

$$\begin{aligned}
 S[U, \varphi] = & \beta_s \sum_{sp} \left(1 - \frac{1}{2} \text{Tr} U_{sp} \right) + \beta_t \sum_{tp} \left(1 - \frac{1}{2} \text{Tr} U_{tp} \right) \\
 & + \sum_x \left\{ \frac{1}{2} \text{Tr} (\varphi_x^+ \varphi_x) + \lambda \left[\frac{1}{2} \text{Tr} (\varphi_x^+ \varphi_x) - 1 \right]^2 \right. \\
 & \left. - \kappa_s \sum_{\mu=1}^3 \text{Tr} (\varphi_{x+\hat{\mu}}^+ U_{x,\mu} \varphi_x) - \kappa_t \text{Tr} (\varphi_{x+\hat{4}}^+ U_{x,4} \varphi_x) \right\}, \quad (1)
 \end{aligned}$$

where $U_{x,\mu}$ denotes the SU(2) gauge link variable, U_{sp} and U_{tp} the path-ordered product of the four $U_{x,\mu}$ around a space-space or space-time plaquette, respectively; φ_x stands for the Higgs field. It is useful to introduce the hopping parameter $\kappa^2 = \kappa_s \kappa_t$ and $\beta^2 = \beta_s \beta_t$. The anisotropies $\gamma_\beta^2 = \beta_t / \beta_s$ and $\gamma_\kappa^2 = \kappa_t / \kappa_s$ are functions of the asymmetry ξ . These functions have been determined with identical results on the one-loop level perturbatively [9] and non-perturbatively [10] demanding the restoration of the rotational symmetry in different physical channels. In this paper we use the specific asymmetry parameter $\xi = 4.052$, which gives $\gamma_\kappa = 4$ and $\gamma_\beta = 3.919$. Details of the simulation techniques can be found in [5].

We choose the parameters as follows. The gauge coupling is set close to its physical value via $\beta = 8$. As it will be discussed later, its renormalized value receives about 15% correction. The scalar self-coupling parameter was chosen to be $\lambda = 1.92 \cdot 10^{-4}$. For the determination of the critical hopping parameter κ_c and the interface tension (see next section) we have used the two-coupling method. The final value for the transition point from this procedure on a $2 \times 24^2 \times 192$ lattice gives $\kappa_c = 0.107791(3)$. To study final volume behaviour we also simulated on a larger lattice, namely $2 \times 32^2 \times 288$, where we obtained $\kappa_c = 0.1077835(25)$.

In order to fix the physical parameters in a numerical simulation, one has to define and compute suitable renormalized quantities at zero temperature. The renormalized gauge coupling can be determined from the static potential of an external SU(2) charge pair, measured by Wilson loops. The physical Higgs mass m_H can be extracted from correlation functions of e.g. $R_x \equiv \frac{1}{2} \text{Tr} (\varphi_x^+ \varphi_x)$ and the φ -link operators $L_{\varphi,x} \equiv \kappa_s \sum_{\mu=1}^3 \text{Tr} (\varphi_{x+\hat{\mu}}^+ U_{x,\mu} \varphi_x) + \kappa_t \text{Tr} (\varphi_{x+\hat{4}}^+ U_{x,4} \varphi_x)$. The W-boson mass m_W can be obtained similarly from the composite link fields ($\varphi_x = \rho_x \cdot \alpha_x$ where α_x is an SU(2) matrix and $\rho_x \geq 0$) $W_{x;rk} \equiv \frac{1}{2} \text{Tr} (\tau_r \alpha_{x+k}^+ U_{x,k} \alpha_x)$, τ_r : Pauli matrices, $r, k = 1, 2, 3$. The connected correlation functions of these operators have been measured in direction of largest extension on two lattices. Note that in principle all numerical estimates for the lightest states in a given channel are only upper bounds. Since at our parameters we are deep in the Higgs phase when simulating the $T = 0$ quantities, the lowest mass is well separated from the vacuum and a cross correlation matrix analysis does not seem to be very essential. The mass fitting was done by the Michael-McKerrel method [11], whose features and application in the SU(2)-Higgs model have been sketched in the fourth reference of [5]. The details of the correlation function and Wilson loop analysis for anisotropic lattice actions can be found in [10].

At $T = 0$ and $\kappa = \kappa_c$ we obtained the following numerical results on $16 \times 8^2 \times 64$ lattices (in units of a_t): the Higgs boson mass is $m_H = 0.2711(51)$ and the W-mass is $m_W = 0.2803(39)$. Combining them with additional data from simulations in the vicinity of κ_c in order to account for

its uncertainty as well, one gets $R_{HW} \equiv m_H/m_W = 0.975(50)$, which corresponds to $m_H = 78(4)$ GeV pole mass, if $m_W = 80$ GeV sets the physical scale. The renormalized gauge coupling comes out to be $g_R^2 = 0.539(16)$. Previous experience [5] shows that the masses and coupling we obtained on the above lattice basically coincide with the infinite volume values within our errors.

3 Thermodynamical quantities and results

Near the endpoint the electroweak phase transition falls into the three dimensional Ising universality class [12], where the two peak structure persists at any finite volume (even at the endpoint). Therefore, we have taken particular attention to study finite volume effects and extrapolate to the infinite volume limit. In view of the large lattices one is confronted with for an extremely weak first order phase transition also in the case of anisotropic lattices, the interface tension σ has been calculated by employing the two-coupling method [13] in κ . This turned out to be robust and most economic in our previous analyses as compared to the histogram or the tunneling correlation length methods [6]. Following refs. [5, 6], the generalization to a situation with anisotropic lattices is straightforward. Namely, if an interface pair perpendicular to the z -direction is enforced by dividing the lattice volume in symmetric and Higgs phases with

$$\kappa = (\kappa_1, \kappa_2) = (\kappa_1 < \kappa_c : z \leq L_t/2, \kappa_2 > \kappa_c : z > L_t/2) \quad (2)$$

as for the κ_c -determination, the related additional free energy ΔF yields for $\Delta\kappa \equiv |\kappa_i - \kappa_c| \ll 1$ the expression

$$a_s^2 a_t \sigma = \lim_{\Delta\kappa \rightarrow 0} \left\{ (\Delta\kappa) \lim_{L_z \rightarrow \infty} L_z \cdot \Delta L_\varphi(\kappa_1, \kappa_2) \right\}, \quad (3)$$

where $L_\varphi^{(i)} = L_\varphi^{(i)}(\kappa_1, \kappa_2)$, $i = 1, 2$, denote the expectation value of the φ -link operators in the respective phases and $\Delta L_\varphi(\kappa_1, \kappa_2) \equiv L_\varphi^{(2)}(\kappa_1, \kappa_2) - L_\varphi^{(1)}(\kappa_1, \kappa_2)$ their difference. Now, since the free energy shift can be shown to behave as $\Delta F \approx \mathcal{O}(\Delta\kappa)$, the $(N+2)$ -parametric Laurent ansätze

$$L_\varphi^{(i)}(\kappa_1, \kappa_2) = -\frac{c_i}{\kappa_i - \kappa_c} + \sum_{j=0}^N \gamma_i^{(j)} (\kappa_i - \kappa_c)^j + \mathcal{O}\left((\Delta\kappa)^{N+1}\right), \quad i = 1, 2 \quad (4)$$

give the finite volume estimator for the interface tension $a_s^2 a_t \hat{\sigma} = L_z (c_1 + c_2)$.

In the left part of figure 1 we illustrate a characteristic two-phase distribution of z -slices for the expectation value $L_\varphi(z)$. An interface pair has developed, and the plateaus marking the pure-phase expectation values $L_\varphi^{(i)}(\kappa_1, \kappa_2)$ are flat and broad enough to ensure that the coexisting phases are stable against any turn-over into one single phase. All simulation data, which were collected in $\kappa = (\kappa_1, \kappa_2)$ centred symmetrically around κ_c for the determination of σ , are listed in table 1. The integrated autocorrelation times of the φ -links are 18 to 160 sweeps for our largest and smallest κ -interval, respectively. Compared to previous analyses on isotropic lattices for stronger first order transitions, the κ -intervals have been chosen closer to each other and to κ_c , while it was always verified that the distinct phases were well separated. At a very weak transition the diverging of $L_\varphi^{(i)}$, when κ_1 (κ_2) approach κ_c from below (above), sets in later and will be less pronounced than for smaller Higgs masses. Therefore, the curvatures in the shapes of the two $L_\varphi^{(i)}$ as functions of κ and particularly their residua should be modelled more accurately in the present case. The least-squares fits to eq. (4) can be done for both φ -links individually or for their difference ΔL_φ . We observed [6] that the second alternative should be preferred. Firstly, correlations between the competing phases give fluctuations in the locations of the interfaces and secondly, a roughening of the interfaces is expected as the phase transition weakens. The two effects are supposed to compensate to some extent in ΔL_φ .

κ_1	κ_2	sweeps	$L_\varphi^{(1)}$	$L_\varphi^{(2)}$	ΔL_φ
0.107761	0.107821	40000	<i>12.7856(73)</i>	<i>21.5913(92)</i>	<i>8.8057(90)</i>
0.107766	0.107816	40000	12.944(11)	21.1656(99)	8.2217(95)
0.107771	0.107811	60000	13.1186(89)	20.7117(90)	7.593(11)
0.107776	0.107806	60000	13.3410(90)	20.215(13)	6.874(12)
0.107781	0.107801	70000	13.711(15)	19.599(16)	5.888(20)
0.107786	0.107796	80000	14.316(39)	18.773(25)	4.457(37)

Table 1: Results for $L_\varphi^{(1)}$, $L_\varphi^{(2)}$ and ΔL_φ for the calculation of σ on a lattice of size $2 \times 24^2 \times 192$, together with their statistical errors from a binning procedure. In order to obtain acceptable χ^2 -values, the entries in italics were only omitted for the four-parameter fits (see text).

In this spirit we carefully examined nearly all types of fits from three- to six-parametric in the Laurent ansätze of eq. (4) for the two kinds of observables $L_\varphi^{(i)}$ and ΔL_φ and for every allowed fit intervals, which could be built up. In part the results on σ might depend on the specific fit interval and on the number of fit parameters in question, but if the inverse-linear part of the general ansatz is supplemented with a fourth or even a fifth fit parameter, the fits are acceptable throughout with tolerable χ^2/dof and can readily be extended over almost the whole range of κ -pairs. In order to control the relevance of a further degree of freedom, we also performed some fits with an additional parameter multiplying the next higher power in $\kappa_i - \kappa_c$. This gave either unreasonably too large χ^2/dof -values, or the error analysis of these fits led to very high statistical errors so that the new fit parameters could not be resolved reliably. As exemplarily displayed in the right diagrams of figure 1 and in figure 2, we found for the best fits $(\hat{\sigma}/T_c^3)_{L_\varphi} = 0.00060(8 + 22)$ from four-parameter χ^2 -fits of $L_\varphi^{(i)}$, $i = 1, 2$, and $(\hat{\sigma}/T_c^3)_{\Delta L_\varphi} = 0.00060(7)$ from the similar fit of ΔL_φ . The quoted error on the former incorporates the statistical error from a bootstrap analysis [14, 6] and an error caused by the uncertainty in κ_c (second entry in parentheses), whereas the solely statistical error on the latter stems from repeated fits with 1000 normally distributed random data around the measured mean values as input.

To study possible finite volume effects and the infinite volume limit, we also simulated on a larger lattice of size $2 \times 32^2 \times 288$ at otherwise unchanged parameters and couplings. The data are displayed in table 2. After an analogous evaluation we obtained for $(\hat{\sigma}/T_c^3)_{L_\varphi} = 0.00062(10 + 25)$ from four-parameter χ^2 -fits of $L_\varphi^{(i)}$, $i = 1, 2$, and $(\hat{\sigma}/T_c^3)_{\Delta L_\varphi} = 0.00063(8)$ from the similar fit of ΔL_φ . These are fully compatible within errors to the preceding results, which indicates that the surface tension does not decrease for increasing volume when the volume is increased by a factor of 2.7. Thus data are compatible with a first order phase transition.

To present our final (infinite volume) value we average all these results to a combined estimate and take their absolute spread including the errors as a measure for the sum of statistical and systematic uncertainties. Assuming all reasonable fits from both spatial volumes to contribute, we finally arrive at

$$\left(\frac{\hat{\sigma}}{T_c^3}\right)_{2-\kappa}^{\text{all}} = 0.0006(4). \quad (5)$$

From quadratic fits of the discontinuities of the order parameters showing up in the thermal cycles of figure 3 for ρ^2 and L_φ (and similarly for the plaquette variables) we also extracted the jump in the Higgs field vacuum expectation value and the latent heat. The jump of the Higgs field vacuum expectation value is given by $\Delta v/T_c = L_t \xi^{-1} \sqrt{2\kappa \Delta \langle \rho^2 \rangle}$ in case of asymmetric lattice spacings. The

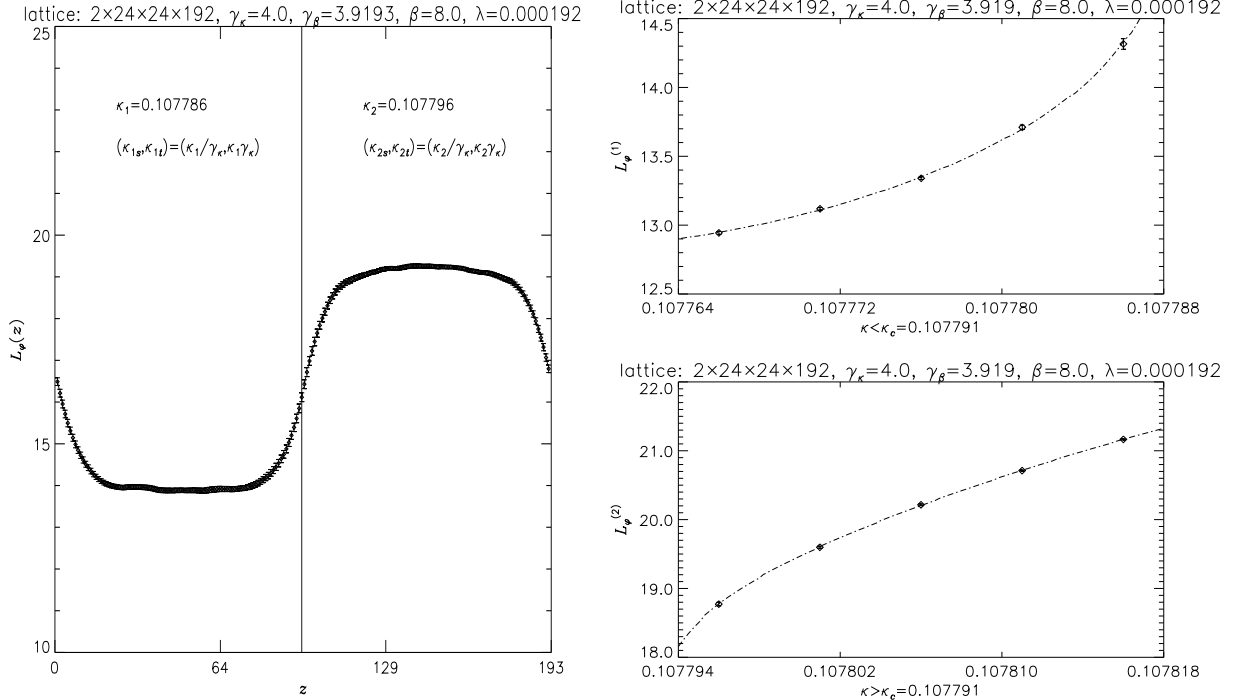


Figure 1: Left: two-phase profile of the z -slice expectation value $L_\varphi(z)$ of L_φ for the smallest κ -interval used in the simulations for the σ -determination in table 1. Right: four-parameter least-squares fits of $L_\varphi^{(i)}$, $i = 1, 2$, separately in each phase. The χ^2 -values are $\chi_1^2 = 2.59$ and $\chi_2^2 = 0.96$, respectively.

latent heat is determined by

$$\frac{\Delta\epsilon}{T_c^4} = \frac{L_t^4}{\xi^3} \frac{\partial\Delta s}{\partial\tau}, \quad (6)$$

where Δ means the jump, s is the average action density and $\tau \equiv -\ln(a_s m_W)$ and the derivative is taken with constant ξ . To determine the partial derivatives of β_s , β_t and λ we have used the perturbative renormalization group equations defining the *lines of constant physics*, while for κ we have followed a procedure similar to the one used in [5] for the isotropic case. We end up with

$$\begin{aligned} \frac{\Delta\epsilon}{T_c^4} = \frac{L_t^4}{\xi^3} \left\{ \frac{1}{\kappa} \frac{\partial\kappa}{\partial\tau} \Delta \langle l_\varphi \rangle + \frac{43}{16\pi^2} g^2 (\beta_s \Delta \langle p_s \rangle + \beta_t \Delta \langle p_t \rangle) \right. \\ \left. + \Delta \langle Q \rangle \left(\frac{2\lambda}{\kappa} \frac{\partial\kappa}{\partial\tau} + \frac{\kappa^2}{4\xi\pi^2} \left[96\lambda_c^2 + \frac{9}{32}g^4 - 9\lambda_c g^2 \right] \right) \right\}, \quad (7) \end{aligned}$$

where $\langle l_\varphi \rangle$ is the average link, $\langle p_s \rangle$ and $\langle p_t \rangle$ are the average plaquette variables, $\langle Q \rangle$ is the average of the quartic part in φ of the lattice action (1) and $\lambda_c = \lambda\xi/(4\kappa^2)$. The results for our simulation parameters are collected in table 3.

4 Estimate for the endpoint for the electroweak phase transition

It is a well known perturbative feature that the finite temperature electroweak phase transition is of first order due to the vanishing magnetic mass (m_T). A non-vanishing parametrization of this

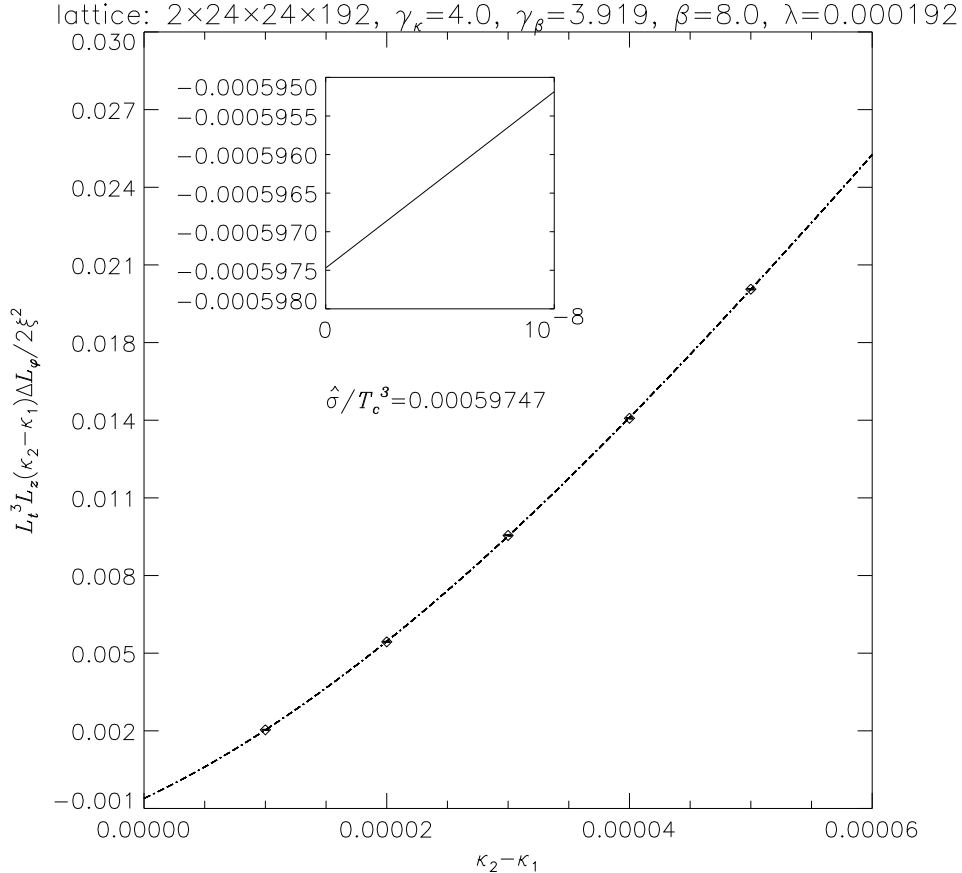


Figure 2: Four-parameter least-squares fit of the φ -link difference ΔL_φ as a function of $\kappa_2 - \kappa_1$ with $\chi^2 = 4.55$. The extrapolation to $\kappa_2 - \kappa_1 = 0$ gives the interface tension.

mass predicts an endpoint $m_{H,c}$ for the first order phase transition. Note that our treatment is purely phenomenological and is performed in one particular gauge, the Landau gauge. The value of the magnetic mass can be obtained e.g. by solving the truncated Dyson-Schwinger equations (gap-equations) [3, 15]. Different treatments of these equations give different numerical values for the magnetic mass. Nevertheless keeping it as an unknown parameter and analysing the behaviour of the different static thermodynamical quantities (e.g. jump of the order parameter, latent heat and interface tension), a scaling behaviour can be observed in the vicinity of $m_{H,c}$ [3]. As we have explicitly checked, this behaviour is essentially independent of the model or loop-order used [4].

We have fitted all our available four-dimensional data at $m_H \approx 19, 35, 49, 80$ GeV (see [5] and the results of the present paper) on the static thermodynamical quantities to the predictions of the one- and two-loop finite temperature effective potential. The perturbative results were considered as a function of one unknown parameter, namely the endpoint of the phase transition $m_{H,c}$ parametrized by a non-vanishing mass in the magnetic sector. The small masses play a less relevant role in the fitting procedure, while the influence of 49 and 80 GeV data on the value of the endpoint is more important. Combining all results (i.e. all masses and thermodynamical quantities), we have seen that at the optimal magnetic mass $\chi^2/\text{dof} \approx 1$, whereas for vanishing m_T the χ^2 -value is considerably larger. This fact can be interpreted as a sign, which indicates the presence of the phase transition endpoint. Our combined value for the endpoint is $m_{H,c} = 106_{-24}^{+88}$ GeV. The estimated value for $m_{H,c}$ is slightly larger than the values of the three-dimensional analyses [8]; however, they are in an approximately $1.5\text{-}\sigma$ agreement. We emphasize that at small L_t 's the phase transition usually tends

κ_1	κ_2	sweeps	$L_\varphi^{(1)}$	$L_\varphi^{(2)}$	ΔL_φ
0.107757	0.107810	10000	12.6839(58)	21.146(12)	8.462(13)
0.107762	0.107805	10000	12.8446(97)	20.708(11)	7.863(13)
0.107767	0.107800	10000	13.026(12)	20.194(19)	7.168(20)
0.107772	0.107795	10000	13.293(17)	19.592(25)	6.299(23)
0.107777	0.107790	10000	13.620(20)	18.752(33)	5.132(31)
0.107780	0.107787	5000	14.075(46)	18.107(54)	4.032(72)

Table 2: Results for $L_\varphi^{(1)}$, $L_\varphi^{(2)}$ and ΔL_φ for the calculation of σ on a lattice of size $2 \times 32^2 \times 288$, together with their statistical errors from a binning procedure.

L_t	T_c/m_H	$\hat{\sigma}/T_c^3$	$\Delta v/T_c$	$\Delta\epsilon/T_c^4$
2	1.86(2)	0.0006(4)	0.37(16)	0.0033(27)

Table 3: Summary of our lattice results at $L_t = 2$ temporal extension.

to be stronger than for larger L_t values [5].

5 Discussion and outlook

Both quantities $\hat{\sigma}/T_c^3$ and $\Delta\epsilon/T_c^4$ for $m_H \approx 80$ GeV are substantially smaller than the perturbative predictions with zero magnetic mass (e.g. $\sigma/T_c^3 \approx 0.002$ [2]). Comparing with our earlier investigations at lower m_H [5, 6], these results confirm the expectation that the interface tension and the latent heat are steeply decreasing functions of the Higgs boson mass, and they are even consistent at $m_H \approx 80$ GeV with a no first order phase transition scenario approximately at the $1\text{-}\sigma$ level.

We have fitted all our four-dimensional data to the perturbative predictions assuming, however, an endpoint for the phase transition parametrized by a phenomenological non-vanishing magnetic mass. Our combined value for the endpoint is $m_{H,c} = 106_{-24}^{+88}$ GeV. Although being in a nearly $1.5\text{-}\sigma$ agreement, the fact that our findings deviate from those of the three-dimensional investigations [8], which claim the endpoint of the first order phase transition line to be at $m_{H,c} \approx 67$ GeV, should be clarified in future.

However, we also have to concede that a temporal lattice extension of $L_t = 2$ may be still too far from the continuum physics. In fact, experience with lattice perturbation theory shows [10] that using anisotropic lattices makes the approach to the continuum limit even slower than for isotropic lattices. So at least some knowledge about the behaviour of the four-dimensional SU(2)–Higgs model at $m_H \approx 80$ and $L_t = 3$ is of principal interest before drawing a final conclusion. Unfortunately the necessary CPU-time requirements to reach an adequate precision on such huge lattices seems not yet to be realistic. Therefore, it would be more desirable to determine the endpoint of the electroweak phase transition on the basis of a study of the Lee-Yang zeros, as applied in refs. [8] to the dimensionally reduced model, within the theory in four dimensions as well.

Acknowledgements

Special thanks go to I. Montvay and G. Münster for essential proposals. Discussions with K. Kajantie, F. Karsch, A. Patkós, M. Shaposhnikov and R. Sommer are also acknowledged. Simulations have

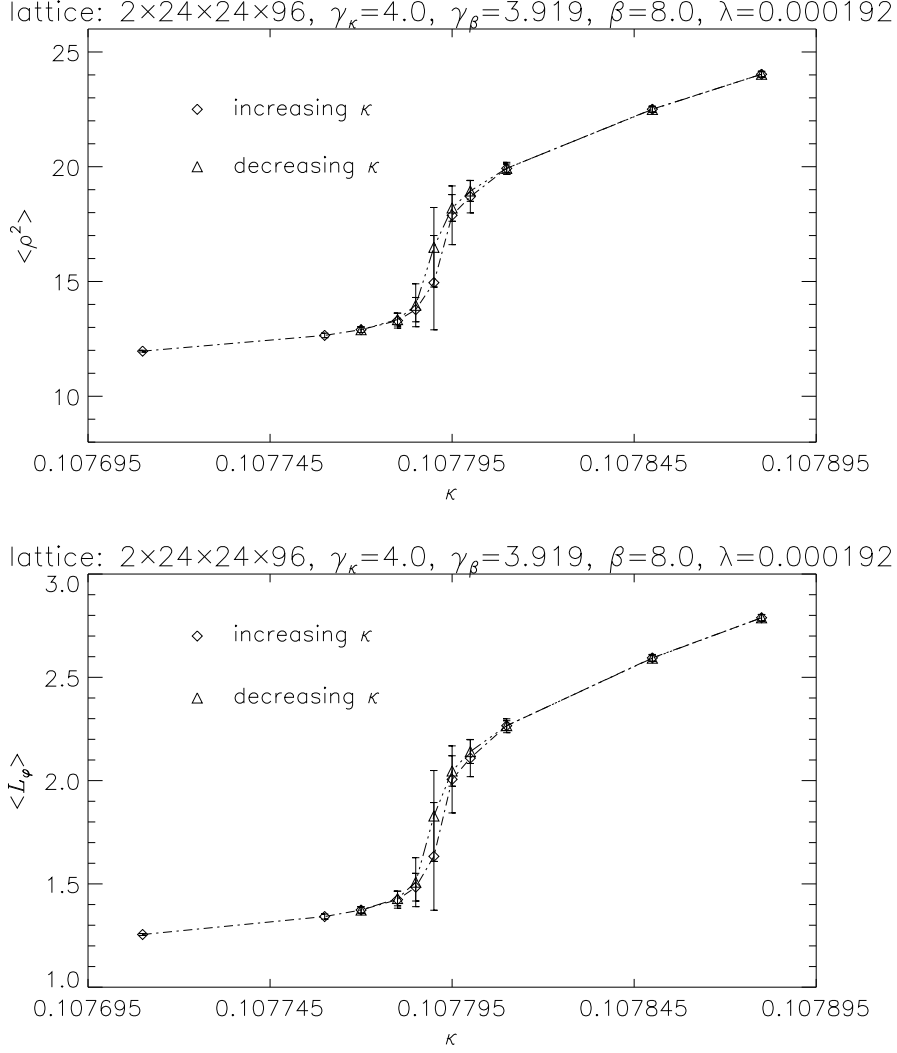


Figure 3: Hysteresis patterns of the operators ρ^2 and L_φ around the critical κ -region at $L_t = 2$.

been carried out on the Cray-T90 at HLRZ-Jülich, on the APE-Quadrics at DESY Zeuthen and on the PMS-8G PC-farm in Budapest. F. Cs. and Z. F. were partially supported by Hung. Sci. Foundation Grants T016240/T022929 and FKFP-0128/1997.

References

- [1] V. A. Kuzmin, V. A. Rubakov, M. E. Shaposhnikov, Phys. Lett. B155 (1985) 36.
- [2] P. Arnold, O. Espinosa, Phys. Rev. D47 (1993) 3546.
- [3] W. Buchmüller, Z. Fodor, T. Helbig, D. Walliser, Ann. Phys. 234 (1994) 260.
- [4] Z. Fodor, A. Hebecker, Nucl. Phys. B432 (1994) 127.
- [5] B. Bunk et al., Nucl. Phys. B403 (1993) 453; Z. Fodor et al., Phys. Lett. B334 (1994) 405, Nucl. Phys. B439 (1995) 147; F. Csikor et al., Nucl. Phys. B474 (1996) 421; Y. Aoki, Phys. Rev. D56 (1997) 3860.

- [6] F. Csikor et al., Phys. Lett. B357 (1995) 156; J. Hein, J. Heitger, Phys. Lett B385 (1996) 242.
- [7] K. Farakos et al., Nucl. Phys. B407 (1993) 356, B425 (1994) 67, B442 (1995) 317; K. Kajantie et al., Nucl. Phys. B466 (1996) 189; O. Philipsen, M. Teper, H. Wittig, Nucl. Phys. B469 (1996) 445.
- [8] K. Kajantie et al., Phys. Rev. Lett 77 1996 (2887); F. Karsch, T. Neuhaus, A. Patkós, J. Rank, Nucl. Phys. Proc. Suppl. 53 (1997) 623; M. Gürtler, E.M. Ilgenfritz, A. Schiller, Phys. Rev. D56 (1997) 3888; for a recent review with references see: M. Laine, in Proc. of the Conf. Strong and Electroweak Matter'97, Eger, Hungary, 21-25 May 1997, World Sci, 1998, p. 160 and hep-ph/9707415.
- [9] F. Csikor, Z. Fodor, Phys. Lett. B380 (1996) 113.
- [10] F. Csikor, Z. Fodor and J. Heitger, hep-lat/9804026.
- [11] C. Michael, Phys. Rev. D49 (1994) 2616; C. Michael, A. McKerrel, Phys. Rev. D51 (1995) 3745.
- [12] K. Rummukainen et al., hep-lat/9805013
- [13] J. Potvin, C. Rebbi, Phys. Rev. Lett. 62 (1989) 3062; S. Huang et al., Phys. Rev. D42 (1990) 2864; Phys. Rev. D43 (1991) 2056 [E].
- [14] B. Efron, Ann. Stat. 7 (1979) 1; SIAM Review 21 (1979) 460.
- [15] W. Buchmüller, O. Philipsen, Nucl. Phys. B 443 (1995) 47; Phys. Lett. B397 (1997) 112.